FINAL REPORT

EARTH SATELLITE ORBIT COMPUTATIONS

8619-6004-TU-000

27 AUGUST 1962

PART II
ATMOSPHERIC EFFECTS

SPACE TECHNOLOGY LABORATORIES, INC.
A SUBSIDIARY OF THOMPSON RAMO WOOLDRIDGE INC.
ONE SPACE PARK • REDONDO BEACH, CALIFORNIA

8619-6004-TU-000

FINAL REPORT

EARTH SATELLITE ORBIT COMPUTATIONS

Part II

ATMOSPHERIC EFFECTS

27 August 1962

Prepared for
National Aeronautics And Space Administration
Goddard Space Flight Center
Greenbelt, Maryland

Under Contract No. NAS 5-1246

Approved:

O. K. Smith

O. K. Smith, Manager
Applied Mathematics Department
Programming and Applied Mathematics Laboratory

SPACE TECHNOLOGY LABORATORIES, INC.
A Subsidiary of Thompson Ramo Wooldridge, Inc.
One Space Park
Redondo Beach, California

ABSTRACT

30452

After a discussion of some currently available model atmospheres, errors in orbital prediction and the optimum selection of smoothing interval are examined. Studies of analytic methods for computing orbits of satellites subject to drag forces are also reported.

Author

ILLUSTRATIONS

Appendix 1

Appendix 2

FINAL REPORT

EARTH SATELLITE ORBIT COMPUTATIONS

Part II - Atmospheric Effects

INTRODUCTION

In this part of the report we will consider several specialized topics relating to the effects of atmospheric density on the computation of satellite orbits. Some of the model atmospheres currently available will first be discussed. Then a theoretical model for the errors in orbital predictions described elsewhere will be compared with the errors in actual predictions for several satellites and applied to estimate the possible improvement which could be made in orbital predictions by introducing a sinusoidal variation into the predictions. Next, the optimum choice of smoothing interval for computing definitive orbits of artificial satellites will be discussed. Finally, we will present the results of efforts to develop a general perturbation method in which drag effects are included. Two papers prepared in the course of this study are included as appendices.

Principal contributors to the study of atmospheric effects have been W. Ganzel and K. Moe.

Editorial responsibility for preparation of the body of the report has been assumed by O. K. Smith.

1. THE MODEL ATMOSPHERES

During the first two years after the launching of Sputnik I, many model atmospheres were proposed. These were all static models because there was as yet little data available. As more data became available it was possible to detect systematic variations and discover some of the correlations which exist between atmospheric density and various solar and geophysical phenomena. As a consequence, most of the model atmospheres proposed in the past two or three years have been dynamic (or time-varying). The leading workers in the construction of these models have been W. Priester, L. G. Jacchia, H. K. Paetzold, and M. Nicolet. The dynamic model atmospheres available in 1961 were compared with the orbital accelerations of EXPLORER VI in the final report on that orbit. None of the models available in 1961 agreed well enough with the observed satellite accelerations to be considered satisfactory. Paetzold's 1962 model [4] became available during the construction of the EXPLORER VI orbit, so it was also compared with the observed accelerations, and it was found to agree within the standard deviation of the derived densities about 70 per cent of the time. Jaccia's new model was not used because it did not include as many known correlations as Paetzold's. Priester and Harris' new model was not yet available when the study was made.

Because of the good agreement between the orbital acceleration of EXPLORER VI and Paetzold's model, this seems to be the most satisfactory model. In it the atmospheric density is a function of the altitude, time of year, local solar time, decimeter solar flux, and geomagnetic planetary amplitude. The first quantities can be derived

from the tracking data, but the last two must be obtained from solar and geomagnetic observatories, respectively. Paetzold's model employs many tables, but polynomials may be fitted to the tabular data in order to reduce the computer storage requirement. Further research is needed to determine how well the decimeter solar flux and geomagnetic planetary amplitude can be predicted, and how best to make such predictions.

During the study of Paetzold's 1962 atmospheric model, several errors and omissions were discovered. In equation (6), the closing parenthesis was omitted after θ_i (h); and the sign before k(200,h) should have been negative. In the second line of equation (6a), a(h) g(a) should probably be a(F, h) g(a).

A_p is expressed in units of 2γ, not γ.

The table of θ_i(h) does not extend as far as is needed. Below 300 km, use θ_{STANL} (h) for θ_i (h). Above 700 km extrapolate linearly.

A comparison of Paetzold's equation (1) with the general expression for rate of change of period reveals that he has assumed that $C_D = 1.813$. Since Paetzold only analyzed satellites which had been aloft for several years, in order to determine the annual effect and the effect of the sunspot cycle, it would be desirable to test his model against the orbital accelerations of various low satellites, such as Sputnik III and its rocket, Atlas-Score, Transit III-B, Ranger I and II, and the two Mercury orbital flights.

2. ERRORS IN ORBITAL PREDICTIONS

The theory of errors in orbital predictions for natural satellites can be traced ultimately to the work of Gauss. The basic assumption in this theory is that the errors are caused by random errors of observation. This is a valid assumption since natural satellites move in drag-free space. Artificial satellites, on the other hand, are subjected to a large and fluctuating atmospheric drag. A theory of errors in orbital predictions for artificial satellites must therefore consider the effect of fluctuating drag, in addition to the observational errors. Such a theory is given in [2] and [3], and is applied to the orbital predictions for the TIROS and Vanguard satellites in Appendix 1.

This theory has also been applied to the problem of determining how much improvement could be made in orbital predictions if the predicted atmospheric density were allowed to vary with the 27 day period which is known to exist in atmospheric density. EXPLORER IV was chosen for the example because data on it was available. The rate of change of period of EXPLORER IV was -2.15×10^{-3} minutes/revolution; the height of perigee was 142 nautical miles; the height of apogee was 1,190 nautical miles; and the period was 109 minutes. The duration of the prediction was N = 165 revolutions, measured from the center of the smoothing interval. The smoothing interval was estimated to be 100 revolutions. The three contributions to the error in an orbital

prediction were calculated from [3] to be: an observational error $O(N) = 2.4 \times 10^{-2}$ minutes, a random error $R(N) = 2.95$ minutes, and a sinusoidal error $S(N) = 2.3$ minutes. The total error found by combining these three contributions, which were considered independent, was $E_{rms}(N) = 3.7$ minutes. (The actual rms error of eight predictions issued by the Vanguard Computing Center was 3.2 minutes.) The theoretical error, with the sinusoidal error removed, was 2.95 minutes. Thus the percentage improvement which could be expected if a sine wave were included in the prediction is 20 per cent. Many satellites now being launched have heights of perigee above 400 nautical miles. The errors in predictions for such satellites (except in the case of balloon satellites, which have a high area to mass ratio) are caused mainly by observational errors, so no improvement could be made by adjusting their drag for the sinusoidal variation.

3. THE CHOICE OF SMOOTHING INTERVAL

If the errors in orbital computations were caused only by observational errors, one would expect that the orbital accuracy could be improved without limit by employing a longer and longer smoothing interval. However, the accuracy of artificial satellite orbits is often made poorer rather than better by increasing the smoothing interval, because of the fluctuating air drag. The choice of a smoothing interval then involves a compromise between introducing unreal fluctuations due to observational errors, and concealing real fluctuations by doing too much smoothing. A theory of the optimum smoothing interval is presented in Appendix 2.

4. DRAG EFFECTS IN GENERAL PERTURBATION METHODS.

While the orbital perturbations produced by drag are very important for many artificial satellites, the perturbations caused by the oblateness of the earth have been much more extensively analyzed, partly because they lend themselves to elegant mathematical treatment. Still, a number of papers dealing with drag alone have appeared, and several of these were examined as a first step toward developing an analytic method for drag and oblateness combined.

The methods proposed by Roberson [5] and Sterne[6,7] were given most attention. Examination of Roberson's paper shows that the theory presented there has several shortcomings. An exponential atmosphere is assumed with the exponent varying linearly with the reciprocal of the distance from the center of the earth. There is no evident distinction between orbits which dip into the atmosphere only near perigee and those which are so nearly circular that they remain within the atmosphere at all times, though osculating elements behave quite differently in the two cases. In addition, there are a number of errors in details of the analysis. Sterne's method is free from these difficulties and also allows the rotation of the atmosphere and the spheroidal shape of the earth to be taken into account, if desired. For these reasons, and because of the favorable experience in computing satellite lifetimes [8] using approximations based on some of Sterne's formulas, we selected Sterne's work as a basis for further analysis and numerical tests.

Brouwer's paper [1] became available after the study was well under way and so was not examined in detail. This seems to be the only work which undertakes to include periodic, as well as secular effects; as a consequence,

the resulting formulas are exceptionally complicated. They deserve further attention, however. In particular, the secular terms should be extracted and compared with those obtained by other methods. Another feature of Brouwer's work is that he is "concerned with the problem of attending to oblateness perturbations and the drag effect in a single solution" whereas other authors treat the two separately and superpose solutions. Of course, superposition is mathematically justifiable as long as each of the perturbations is not carried beyond the first order terms of an expansion in some small parameter.

5. NUMERICAL TESTS OF STERNE'S METHOD

In his analysis, Sterne introduces an osculating exponential atmosphere with density given by

$$\rho = \rho_{\pi} \exp\left[-K(h-h_{\pi})\right]$$

where ρ_{π} = density at pericenter

h = height

h_{π} = height of pericenter

The reciprocal of the constant K is sometimes referred to as the "scale height". With c=Kae and the usual notation for orbital elements, expressions for the secular rate of change of the elements are developed in two forms; one to be used when c is greater than (roughly) two and another valid for small c. For c greater than two, formulas given in [6] allow computation of secular rates of all elements, omitting effects of planetary flattening. These formulas have been tested by comparison with a Cowell numerical integration of an orbit approximating that of Atlas-Score. Dynamical effects in the atmosphere and gravitational effects of oblateness, sun, moon, etc. were not included since the objective was to see whether Sterne's analysis adequately approximated his model.

Results appear in Tables 1 and 2. Elements, and from them coordinates, were computed at intervals of 100.14 minutes, approximately the period of the satellite, by a simple recursion of the form

$$e(t_{n+1}) = e(t_n) + (t_{n+1}-t_n)\dot{e}_{sec}(t_n)$$

where $\dot{e}_{sec}$ is the secular rate given by formulas from [6]. In the last column of Table 1 will be found Δr, the square root of the sum of the squares of the difference between the Sterne and Cowell coordinates. Two points about the results seem worth mentioning. First, these errors correspond to timing errors of a half second or so and are consequently a couple of orders of magnitude below the random and sinusoidal errors discussed in Section 2. They are probably comparable to the errors inherent in any method which omits periodic effects. Secondly, there is no perceptible secular trend in Δr, indicating that the method adequately accounts for the dominant effects.

For the final time, at the end of about nineteen revolutions, Table 2 compares osculating elements calculated two ways. Values are also given at the epoch, not only to define the orbit, but also to show that some elements vary significantly from their initial values.

TABLE 1

n	t (min)	M (degrees)	Δr (feet)
1	100.14	- .334	15731.
2	200.28	- .598	15935.
3	300.42	- .791	16233.
4	400.56	- .914	16599.
5	500.70	- .966	17018.
6	600.84	- .948	17464.
7	700.98	- .859	17913.
8	801.12	- .699	18333.
9	901.26	- .469	18706.
10	1001.40	- .168	18994.
11	1101.54	.204	19183.
12	1201.68	.647	19240.
13	1301.82	1.161	19144.
14	1401.96	1.746	18867.
15	1502.10	2.402	18384.
16	1602.24	3.130	17672.
17	1702.38	3.928	16704.
18	1802.52	4.798	15458.
19	1902.66	5.739	13912.

TABLE 2

	t = 0	t = 1902.66		Diff.
		STERNE	COWELL	
a (feet)	23452296.	23393955.	23393335.	620.
e	.08452	.0822428	.0822956	- .000528
i (degrees)	32.305	32.303219	32.303216	.000003
Ω (degrees)	206.240	206.24083	206.24070	.00013
ω (degrees)	167.000	166.99925	166.99874	.00051
E (degrees)	+ .305 x 10^{-6}	6.291406	6.257795	.033611
M (degrees)	.279 x 10^{-6}	5.739309	5.743829	- .00452
P (mins)	100.24278	99.86896	99.86499	.00397

6. EXTENSION OF STERNE'S FORMULAS

In [6], Sterne developes an expression (12a) for the secular rate of change of period due to drag, assuming $c < 2$ and making allowance for planetary flattening. This section extends his work by driving corresponding formulas for the other elements: semi-major axis a, eccentricity e, angle of inclination i, longitude of ascending node Ω, and argument of perigee ω.

From [6], p. 780, we have

$$\rho = \rho_\pi \, e^{-c(1-\cos E)} \left[1 + \frac{q_1 \sin^2 E}{(1-e\cos E)^2} + \frac{q_2 \sin^4 E}{(1-e\cos E)^4} + \dots \right]$$

$$+ \rho_\pi \, e^{-c(1-\cos E)} \, G(E)$$

where

G(E) is an odd function of E

ρ is the density of the atmosphere at height h

ρ_π is the density at perigee

$$q_1 = (1-e^2)\left[-q\cos 2\omega + (q^2/2)\sin^2 2\omega\right]$$

$$q_2 = (1-e^2)^2 (q^2/2)\cos 4\omega$$

$$q = K a_o f \sin^2 i$$

$f = \frac{a_o - b_o}{a_o}$, a_o and b_o being the planets equatorial and polar radii respectively

$= 3.35232987 \times 10^{-3}$ for the earth

Since each of the expressions for the orbital elements contains an integral of the form

$$\int_0^{2\pi} \rho\, F(E)\, dE$$

and in each case F(E) is an even function of E, we need not concern ourselves with G(E), the odd part of the expansion of ρ.

By definition $I_n(x)$ is the Bessel function of imaginary argument

$$I_n(x) = i^{-n} J_n(ix) = \frac{1}{\pi}\int_0^{\pi} e^{x \cos y} \cos(ny)\, dy$$

By using recursion relations, any $I_n(c)$ can be reduced to a sum of $I_0(c)$ and $I_1(c)$.

The secular charge in semi-major axis follows readily from Sterne's formula (12d) and the relationship between a and P. After a little manipulation, there results

$$\dot{a}_{sec} = -2\mu^{1/2}(1-d)^2\, b\, a^{1/2}\, e^{-c}\, \rho_{\pi}\, [B_0 I_0(c) + B_1 I_1(c)]$$

where

$$b = \frac{C_D A}{2m}$$

C_D is the dimensionless aerodynamic drag coefficient.

A is the cross sectional area of the satellite

m is the mass of the satellite

$$B_0 = 1 + e^2\left(j^2 + \frac{1}{2}\right) - j\frac{e^3}{c} + q_1 \frac{e}{c}\left[2(j+1) - \frac{3e}{c}\left(j^2+4j+\frac{7}{2}\right)\right] + q_2 \frac{3}{c^2}\left(1 - \frac{8e}{c}(j+2)\right)$$

$$B_1 = 2ej - \frac{e^2}{c}\left(j^2+\frac{1}{2}\right) + \left(1+\frac{2}{c^2}\right)je^3 + q_1 \frac{1}{c}\left[1 - \frac{4e}{c}(j+1) + e^2\left(1+\frac{6}{c^2}\right)\left(j^2+4j+\frac{7}{2}\right)\right]$$
$$- q_2 \frac{6}{c^2}\left[\frac{1}{c} - \left(1+\frac{8}{c^2}\right)e(j+2)\right]$$

up to but not including terms in e^4, $q_1 e^3$, $q_2 e^2$
where

$$j = \frac{1+d}{1-d}$$

$$d = \frac{\omega_s}{n} (1-e^2)^{1/2} \cos i$$

From (3a) of the reference we have for the secular rate in eccentricity

$$\dot{e}_{sec} = - (1-e^2) \frac{abn}{\pi} \int_0^{2\pi} \rho F_e(E) dE$$

where

$$F_e(E) = \left[\frac{1+e \cos E}{1-e \cos E}\right]^{1/2} (1-d \frac{1-e \cos E}{1+e \cos E}) \left[\cos E - \frac{d}{2(1-e^2)} (1-e \cos E) \times (2 \cos E - e - e \cos^2 E)\right]$$

Expanding $F_e(E)$ and keeping terms up to and including e^3, we obtain

$$F_e(E) = \frac{1}{2(1-e^2)} \left[2(1-d)^2 \cos E + e (1-d) \left\{d + (5d+2) \cos^2 E\right\} + e^2 \left\{2(d^2+d-1) \cos E + (5d^2+1) \cos^3 E\right\} + \frac{e^3}{2} \left\{- (3d^2+5d+4) \cos^2 E + (2+d-7d^2) \cos^4 E\right\} + \ldots\right]$$

Now $F_e(E)$ is an even function of E, so when we multiply $F_e(E)$ by the even part of the expansion of ρ, we obtain for the integrand, $F_1(E)$

$$F_1(E) = e^c \cos E \left[J_{oe} + q_1 J_{1e} + q_2 J_{2e}\right]$$

where

$$J_{oe} = 2(1-d)^2 \cos E + e(1-d)\left\{d + (5d+2)\cos^2 E\right\}$$
$$+ e^2\left\{2(d^2+d-1)\cos E + (5d^2+1)\cos^3 E\right\}$$
$$+ \frac{e^3}{2}\left\{-(3d^2+5d+4)\cos^2 E + (2+d-7d^2)\cos^4 E\right\}$$
$$+ \ldots$$

$$J_{1e} = 2(1-d)^2(\cos E - \cos^3 E) + e(1-d)\left[d + 6\cos^2 E - (d+6)\cos^4 E\right]$$
$$+ e^2\left[2(2d-1)\cos E + (d^2-10d+13)\cos^3 E - (d^2-6d+11)\cos^5 E\right]$$
$$+ \ldots$$

$$J_{2e} = 2(1-d)^2(\cos E - 2\cos^3 E + \cos^5 E)$$
$$+ e\left\{d(1-d) + 5(d^2-3d+2)\cos^2 E - (7d^2-27d+20)\cos^4 E\right.$$
$$\left. + (3d^2-13d+10)\cos^6 E\right\}$$
$$+ \ldots$$

And our expression for $\dot{e}_{sec}$ becomes

$$\dot{e}_{sec} = -\frac{abn}{2}\rho_x e^{-c}\ \frac{1}{\pi}\int_0^{2\pi} F_1(E)dE$$

Expressing $F_1(E)$ in terms of cosines of multiple angles, we have

$$J_{oe} = 2(1-d)^2 \cos E + \frac{e}{2}(1-d)\left[7d + 2 + (5d+2)\cos 2E\right]$$
$$+ \frac{e^2}{4}\left[(23d^2+8d-5)\cos E + (5d^2+1)\cos 3E\right]$$
$$- \frac{e^3}{16}\left[33d^2 + 17d + 10 + 8(5d^2+2d+1)\cos 2E + (7d^2-d-2)\cos 4E\right]$$
$$+ \ldots$$

$$J_{1e} = \frac{1}{2}(1-d)^2(\cos E - \cos 3E) + \frac{e(1-d)}{8}\left[5d + 6 - 4d\cos 2E - (d+6)\cos 4E\right]$$
$$+ \frac{e^2}{16}\left[2(d^2+2d+7)\cos E - (d^2+10d+3)\cos 3E - (d^2-6d+11)\cos 5E\right]$$
$$+ \ldots$$

$$J_{2e} = \frac{1}{8}(1-d)^2(2\cos E - 3\cos 3E + \cos 5E)$$
$$+ \frac{e}{32}(1-d)\left\{2(10+3d) - (10+13d)\cos 2E - 10(2-d)\cos 4E\right.$$
$$\left. + (10-3d)\cos 6E\right\}$$
$$+ \ldots$$

Noting that $F_1(E)$ is an even function we may write the integral as

$$\dot{e}_{sec} = -abn\,\rho_\pi\, e^{-c}\,\frac{1}{\pi}\int_0^\pi F_1(E)dE$$

And using the definition of the Bessel function, we may integrate term by term to obtain

$$\dot{e}_{sec} = -abn\,\rho_\pi\, e^{-c}\left\{D_{oe} + q_1 D_{1e} + q_2 D_{2e} + \ldots\right\}$$

where

$$D_{oe} = 2(1-d)^2 I_1(c) + \frac{e}{2}(1-d)\left[(7d+2) I_o(c) + (5d+2) I_2(c)\right]$$
$$+ \frac{e^2}{4}\left[(23d^2+8d-5) I_1(c) + (5d^2+1) I_3(c)\right]$$
$$- \frac{e^3}{16}\left[(33d^2+17d+10) I_o(c) + 8(5d^2+2d+1) I_2(c) + (7d^2-d-2) I_4(c)\right]$$
$$+ \ldots$$

$$D_{1e} = \frac{1}{2}(1-d)^2(I_1(c)-I_3(c)) + \frac{e(1-d)}{8}\left[(5d+6)I_o(c) - 4d I_2(c)-(d+6) I_4(c)\right]$$
$$+ \frac{e^2}{16}\left[2(d^2+2d+7) I_1(c) - (d^2+10d+3) I_3(c) - (d^2-6d+11) I_5(c)\right]$$
$$+ \ldots$$

$$D_{2e} = \frac{1}{8}(1-d)^2\left[2I_1(c) - 3I_3(c) + I_5(c)\right]$$
$$+ \frac{e}{32}(1-d)\left[2(10+3d) I_o(c) - (10+13d) I_2(c) - 10(2-d) I_4(c)\right.$$
$$\left. + (10-3d) I_6(c)\right]$$
$$+ \ldots$$

Now we wish to reduce $D_{oe} + q_1 D_{1e} + q_2 D_{2e}$ to the form $B_{oe} I_o(c) + B_{1e} I_1(c)$, so we apply the recursion relations for $I_n(c)$ and we obtain

$$\dot{e}_{sec} = - abn \rho_x e^{-c}\left\{B_{oe} I_o(c) + B_{1e} I_1(c)\right\}$$

where

$$B_{oe} = 2e(1-d)(3d+1) - \frac{e^2}{c}(5d^2+1) - e^3\left\{5d^2 + 2d + 1 + \frac{3}{2c^2}(7d^2-d-2)\right\}$$
$$+ \frac{q_1}{c}\left[2(1-d)^2 - \frac{3e(1-d)(d+6)}{c} + e^2\left\{d^2-2d+9+\frac{12}{c^2}(d^2-6d+11)\right\}\right]$$
$$- \frac{6(1-d)q_2}{c^2}\left[\frac{4(1-d)}{c} - e\left\{5-d+\frac{10(10-3d)}{c^2}\right\}\right]$$

$$B_{1e} = 2(1-d)^2 - \frac{e}{c}(1-d)(5d+2) + e^2\left\{7d^2+2d-1+\frac{2}{c^2}(5d^2+1)\right\}$$
$$+ \frac{e^3}{2c}\left\{d(17d+3) + \frac{6}{c^2}(7d^2-d-2)\right\}$$
$$- \frac{q_1}{c}\left[\frac{4(1-d)^2}{c} - 2e(1-d)\left\{d+3+\frac{3}{c^2}(d+6)\right\}\right.$$
$$\left. + \frac{e^2}{c}\left\{5d^2-22d+51+\frac{24}{c^2}(d^2-6d+11)\right\}\right]$$
$$+ \frac{3(1-d)q_2}{c^2}\left[2(1-d)\left(1+\frac{8}{c^2}\right) + \frac{e}{c}\left\{19d-70-\frac{40(10-3d)}{c^2}\right\}\right]$$

Development of formulas for the elements i and Ω proceeds in much the same way, so details will be omitted. Assembling results, we have

$$\left(\frac{di}{dt}\right)_{sec} = -\frac{1}{2}\,ab\omega_s \sin i \,\frac{1}{(1-e^2)^{1/2}}\,\rho_\pi\, e^{-c}\left[B_{oi}\, I_o(c) + B_{1i}\, I_1(c)\right]$$

where

$$B_{oi} = (1-d)(1+W) - \frac{4c}{c}Wd + \frac{e^2}{2}\left[(1+W)(1-13d) - \frac{6W(1+3d)}{c^2}\right]$$

$$- \frac{e^3}{c}\left[1 + W + 6d + 4\,Wd\,(1 + \frac{6}{c^2})\right]$$

$$+ \frac{q_1}{c}\left[-\frac{6(1-d)W}{c} + 2e\left\{d(1+W) + \frac{24W}{c^2}\right\} + \frac{3e^2}{2c}\left\{3d+1-W(5-d)(1+\frac{40}{c^2})\right\}\right]$$

$$+ \frac{3q_2}{c^2}\left[(1-d)\left\{1+W(1+\frac{40}{c^2})\right\} - \frac{4e}{c}\left\{2+12W-5Wd+\frac{120W(2-d)}{c^2}\right\}\right]$$

$$B_{1i} = \frac{-2(d-1)W}{c} + 2e\left[2d - (W+1) + 2Wd\,(1 + \frac{2}{c^2})\right]$$

$$- \frac{e^2}{2c}\left[1 - 13d - W(1+3d)(5+\frac{12}{c^2})\right]$$

$$+ e^3\left[(W+1)(6d+1) + \frac{2}{c^2}(1+W+6d+7Wd) + \frac{48Wd}{c^4}\right]$$

$$+ \frac{q_1}{c}\left[(1-d)\left\{1+W(1+\frac{12}{c^2})\right\} - \frac{4e}{c}\left\{d(1+W) + 3W(1+\frac{8}{c^2})\right\}\right.$$

$$\left. - \frac{1}{2}e^2\left\{(1+3d)(1+W+\frac{6}{c^2}) + \frac{12W}{c^2}(d-5)(3+\frac{20}{c^2})\right\}\right]$$

$$- \frac{6q_2}{c^2}\left[\frac{(1-d)}{c}\left\{1 + 2W(3+\frac{20}{c^2})\right\}\right.$$

$$\left. - e\left\{1 + W + \frac{8}{c^2}(1 + 21W - 10Wd + \frac{60W(2-d)}{c^2})\right\}\right]$$

where

$$W = \cos 2\omega$$

$$\dot{\Omega}_{sec} = - \frac{ab\omega_s \sin 2\omega}{2(1-e^2)^{1/2}}\; e^{-c\rho_\pi}\left[B_{o\Omega}\, I_o(c) + B_{1\Omega}\, I_1(c)\right]$$

where

$$B_{o\Omega} = 1-d - \frac{4ed}{c} + \frac{e^2}{2}\left[1-13d - \frac{6(1+3d)}{c^2}\right] - \frac{e^3}{c}\left[1+4d\left(1+\frac{6}{c^2}\right)\right]$$
$$+ \frac{q_1}{c}\left[\frac{6(d-1)}{c} + 2e\left(d+\frac{24}{c^2}\right) + \frac{3e^2}{2c}(d-5)\left(1+\frac{40}{c^2}\right)\right]$$
$$+ \frac{3q_2}{c^2}\left[(1-d)\left(1+\frac{40}{c^2}\right) - \frac{4e}{c}\left\{12-5d + \frac{120(2-d)}{c^2}\right\}\right]$$

$$B_{1\Omega} = \frac{2(d-1)}{c} - 2e\left[1-2d\left(1+\frac{2}{c^2}\right)\right] + \frac{e^2}{2c}(1+3d)\left(5+\frac{12}{c^2}\right)$$
$$+ e^3\left[1 + 6d + \frac{2}{c^2}\left(1+7d+\frac{24d}{c^2}\right)\right]$$
$$+ \frac{q_1}{c}\left[(1-d)\left(1+\frac{12}{c^2}\right) - \frac{4e}{c}\left\{d + 3\left(1+\frac{8}{c^2}\right)\right\} - \frac{e^2}{2}\left\{3d+1 - \frac{12}{c^2}(5-d)\left(3+\frac{20}{c^2}\right)\right\}\right]$$
$$+ \frac{6q_2}{c^2}\left[\frac{2(d-1)}{c}\left(3+\frac{20}{c^2}\right) + e\left\{1+\frac{8}{c^2}(21-10d) + \frac{480}{c^4}(2-d)\right\}\right]$$

The relationship between argument of perigee and longitude of the node gives at once

$$\dot{\omega}_{sec} = -\cos i\, \dot{\Omega}_{sec}$$

as in (6) of the reference.

This completes the set of formulas for small c, including planetary flattening. For a spherical earth, they may be simplified by setting $q = q_1 = q_2 = 0$. Further study of these results is needed, along with numerical tests like those reported in the preceding section. Some investigation and experimentation will be required to establish the range of the parameter c for which each method is valid and to ascertain whether these ranges meet or overlap.

REFERENCES

1. Brouwer, D., and Hori, G., "Theoretical Evaluation of Atmospheric Drag Effects on the Motion of an Artificial Satellite," Astronomical Journal, 66 (1961) pp 193-225.
2. Moe, K., "A Model for the Errors in Satellite Orbit Predictions Caused by Fluctuations in Drag," Space Technology Laboratories, Inc. Report 600-0000-09145, April 1960.
3. Moe, K., "Stochastic Models of the Errors in Orbital Predictions for Artificial Earth Satellites," (to appear in the ARS Journal).
4. Paetzold, H. K., "Model for the Variability of the Terrestrial Atmosphere above 150 km after Satellite Observation," University of Cologne, 1961.
5. Roberson, R. E., "Air Drag Effect on a Satellite Orbit Described by Difference Equations in the Revolution Number," Quarterly of Applied Mathematics 16 (1958) pp 131-136.
6. Sterne, T. E., "Effect of the Rotation of a Planetary Atmosphere upon the Orbit of a Close Satellite," ARS Journal, 29 (1959) pp 777-782.
7. Sterne, T. E., "An Introduction to Celestial Mechanics," Interscience Publishers, Inc., New York, 1960.
8. Wolverton, R. E. (ed.),"Flight Performance Handbook for Orbital Operations," Space Technology Laboratories, Inc., Redondo Beach, California, 1961.

PART II

APPENDIX 1

ERRORS IN ORBITAL PREDICTIONS FOR METEOROLOGICAL AND GEODETIC SATELLITES

by

Kenneth Moe

Part II

APPENDIX 1

ERRORS IN ORBITAL PREDICTIONS FOR METEOROLOGICAL AND GEODETIC SATELLITES

The atmosphere traversed by artificial satellites fluctuates in density, in response to solar activity. This fact was discovered by Priester [1], and has been confirmed and amplified by many workers [2, 3]. The fluctuations in atmospheric density are one cause of errors in orbital predictions [4, 5, 6, 7], and they also introduce an ambiguity into the determination of definitive orbits [8]. Knowledge of these density fluctuations has been used to construct a theoretical model [4, 5] of errors in orbital predictions. In this appendix the errors in orbital predictions for meteorologic and geodetic satellites will be computed from the model and compared with errors in actual predictions.

The theoretical model was derived from orbital acceleration of the early satellites such as Sputnik III and Vanguard I. Data on the accelerations of satellites have continued to accumulate; some of the best data have been derived by Jacchia and Slowey [9] from the observations of the balloon satellite, EXPLORER IX. Their data are shown in Figure 1a, in which the upper curve shows the rates of change of period caused by atmospheric drag, and the lower curve shows the rates of change of period caused by solar radiation pressure. The autocorrelation function [10] of the drag fluctuations is shown in Figure 1b. A periodicity of approximately 27 days, which is correlated with the motion of active regions across the solar disk, is evident in the autocorrelation function. The "short-term autocorrelation function" in Figure 1c was obtained by removing the 27 day periodicity and trend from the orbital acceleration, and computing the autocorrelation function of the drag fluctuations which remained.* Figures 1b and 1c illustrat

---

* The indicated correlation time of one or two days is an upper bound, because correlations are introduced by the procedure for deriving the orbital accelerations.

the two components of drag variation which were used in constructing the theoretical model for errors in orbital predictions; a 27-day sinusoidal variation and a short-term ("random") fluctuation. A third source of error in predictions is the errors in the tracking observations.

In the model for the errors in orbital predictions the root-mean-square error, S (N), caused by the sinusoidal variation in atmospheric density is given by

$$S(N) = \frac{A}{k^2} \sqrt{\frac{\alpha^2 + \beta^2}{2}} \qquad (1)$$

where

$$\alpha = \cos(kN) - \frac{2}{ik} \sin\left(\frac{ik}{2}\right) + \frac{64}{i^3 k}\left[N^2 - \frac{i(i+2)}{12}\right]\left[1 - \cos\left(\frac{ik}{4}\right)\right]\sin\left(-\right.$$

$$\beta = \sin(kN) - kN + \frac{8N}{ik(i+2)}\left[\cos\left(\frac{ik}{2}\right) - 1 + \frac{i^2 k^2}{8}\right]$$

and

$$A = 5.2\, h_p \left|D\right| \times 10^{-4}$$

where h_p is the height of perigee in kilometers, D is the smoothed rate of change of period (in minutes per revolution), i is the number of revolutions over which observations were smoothed to derive the orbital elements and rate of change of period, $k = 2\pi P/27$ (where P is the period in days), and N is the duration of the predictions measured in revolutions from the center of the smoothing interval.

The rms error, R (N), caused by random drag fluctuations is

$$R(N) = F \left\{ \frac{N^3}{3} + 2 \left(\frac{i}{u}\right)^3 \left[\frac{64}{5} \left(\frac{N}{i}\right)^4 - 16 \left(\frac{N}{i}\right)^3 + \left(\frac{N}{i}\right)^2 \right] \right\}^{1/2} \quad (2$$

r $N \geq i/2 >> 1$

ere $F = 3.1\, h_p \left| D \right| \times 10^{-3}$. Within the smoothing interval ($N < \frac{i}{2}$), the expression r the random error is more complicated, but can be calculated by the methods used in pendices D and G of Reference 4.

The rms error, O (N), caused by errors in the tracking observations, is

$$O(N) = \frac{\sigma_o}{i^2\sqrt{M}} \left\{ \begin{array}{l} i^4 \left[\frac{M}{M+2} + \frac{16}{9} \left(\frac{M+2}{M}\right)^2 \right] + 32\, Ni \left[\frac{i^2}{3M} - \frac{4N^2}{M+2} \right] \\ + 256\, N^4 + 16 N^2 i^2 \left[\frac{M}{M+2} - \frac{8}{3} \left(\frac{M+2}{M}\right) - \frac{2M}{(M+2)^2} \right] \end{array} \right\}^{1/2} \quad (3$$

ere M is the number of independent observations in the smoothing interval of i revolutions σ_o is the equivalent observational error in minutes of time. The equivalent observational error of a "semi-smooth" Minitrack observation is about 0.008 minutes of time. re is approximately one semi-smooth Minitrack observation per revolution of the satellit

On the assumption that the three errors are mutually independent, the total rms error an orbital prediction is

$$E(N) = \left\{ \left[R(N)\right]^2 + \left[S(N)\right]^2 + \left[O(N)\right]^2 \right\}^{1/2} \quad (4)$$

The errors in orbital predictions for Vanguard I near the time of sunspot maximum been computed from equations (1), (2), (3), and (4). They are graphed in Figure 2 as nction of the duration of the prediction, and compared with the rms error of twenty ictions issued by the Vanguard Computing Center in the Autumn of 1958. The smoothing

interval was 89 revolutions. Notice that the errors did not change greatly within the smoothing interval ($N \leq i/2 = 45$ revolutions), but increased rapidly outside.

Figure 3 shows a different kind of graph in which the error at the end of a one or two-week prediction for Vanguard I, issued by Vanguard and NASA computing centers, is plotted as a function of the year in which the prediction was made. Because of oblateness perturbations and the motion of the earth in its orbit, the position of perigee of Vanguard I moves in and out of the sunlight with a period of several years. The air drag is much larger in the sunlit hemisphere than in the dark hemisphere [1, 2, 3]. Since the fluctuations in atmospheric density are assumed in the model to be proportional to the atmospheric density itself, the errors then should vary with a period of several years. Superimposed on this periodic variation is a slower downward trend due to the decrease in air density correlated with the waning of the sunspot cycle. It can be seen from the graph that as perigee passed from sunlight to twilight and into darkness the errors decreased, and the errors increased again as perigee passed back into the sunlight. However, the actual errors in sunlight in 1961 were approximately twice as large as the theoretical model gave. This suggests that the percentage fluctuations in atmospheric density have actually increased since 1958 instead of remaining constant, as the model assumes, or even declining with solar activity as one might guess. It would be desirable to see whether a long series of predictions for any other satellite exhibits this unexpected behavior, but no other long series is available to the author. When perigee was in the sunlight the errors in predictions for Vanguard I were caused mainly by drag fluctuations, but when perigee was in darkness the errors were caused mainly by observational errors of the Minitrack system. (The curve for observational error in Figure 3 was higher in 1961 than in 1958 because the duration of the predictions was increased.)

Figure 4 shows the errors in the one-to two-week orbital predictions tangential
the path of the Tiros weather satellites, as a function of the number of revolutions
om the center of the smoothing interval. The Tiros I, II, and III satellites had
ry similar orbits. The theoretical curve for only one of them is shown because
e theoretical curves differ less than the actual errors do. The Tiros satellites
re so high that the errors in predictions for them were caused almost entirely by
e observational errors of the Minitrack stations. The root-mean-square errors of groups
actual predictions for the three Tiros satellites are indicated by the circle,
angles, and square in Figure 4. An error of 0.1 minute of time is equivalent to a
itional error of approximately 40 kilometers tangential to the path. The errors at
ght angles to the path are an order of magnitude smaller.

Some of the meteorologists who work with the TIROS weather pictures would like to
the predictions to locate points on the pictures with better accuracy. When points
the ground can be recognized in the photographs, the clouds can be located by photo-
ammetric means with better accuracy than the accuracy of the orbital prediction. But
n the surface features are unrecognizable, the clouds must be located by combining the
dicted orbital position with the orientation of the satellite axes. The standard
iation of the orbital position varies from 1/2 to 40 kilometers along the satellite's
, and is an order of magnitude smaller at right angles to the path.

When ground points are unrecognizable, there are three sources of attitude information
rared sensors placed at 90° to the spin axis, infrared sensors placed at 45° to the
n axis, and a mathematical model which uses the magnetic moment, gravity gradient,
eddy currents. The mathematical model can be used along with other attitude data [11]

An examination of the Tiros III attitude during July and August 1961 computed by Natrella indicated that the standard deviations of the right ascension and declination of the spin axis were 2° and 3°, respectively. At a slant range of 1,000 kilometers, and error of 3° causes a positional error of 47 kilometers. Thus the orbital prediction and the attitude determination can both produce errors of approximately 40 kilometers, which it would be quite difficult to reduce. The best hope of locating clouds with better accuracy, in the opinion of the writer, lies in exploiting the method of variable development of the Tiros photographs, as described by Mendoza and Vasques [12] of General Dynamics - Astronautics.

REFERENCES

[1] W. Priester and H. A. Martin, Mitteilung der Universitats-Sternwarte Bonn, No. 29, 1960.

[2] H. K. Paetzold, Model for the Variability of the Terrestrial Atmosphere Above 150 km after Satellite Acceleration, University of Cologne, 1962.

[3] L. G. Jacchia, Nature, 192, No. 4808, p. 1147, 23 December 1961.

[4] K. Moe, A Model for the Errors in Satellite Orbital Predictions Caused by Fluctuations in Drag, Space Technology Laboratories Report 60-0000-09145, April 1960.

[5] K. Moe, Stochastic Models of the Errors in Orbital Predictions for Artificial Earth Satellites (To appear in the ARS Journal).

[6] K. Moe, Nature 192, 151, 14 October 1961.

[7] H. K. Karrenberg, E. Levin, and D. H. Lewis, Variation of Satellite Position with Uncertainties in the Mean Atmospheric Density, ARS Journal, 32, 576 (1962

[8] K. Moe, in SPACE RESEARCH III (Satellite Geodesy, Edited by G. Veis), North-Holland Publishing Co., Amsterdam (to be published, 1962).

[9] L. G. Jacchia and J. W. Slowey, Smithsonian Astrophysical Observatory, Special Report No. 84, February 1962.

[10] J. L. Lawson, and G. E. Uhlenbeck, Threshold Signals, McGraw-Hill Book Co., New York, 1947.

[11] J. V. Natrella, Private Discussion of Tiros Attitude, Goddard Space Flight Center, 19 March 1962.

[12] B. A. Mendoza, and T. Vasques, Automatic Processing and Display of Meteorological-Satellite Television Data, American Geophysical Union Meeting, Washington, 25-28 April 1962.

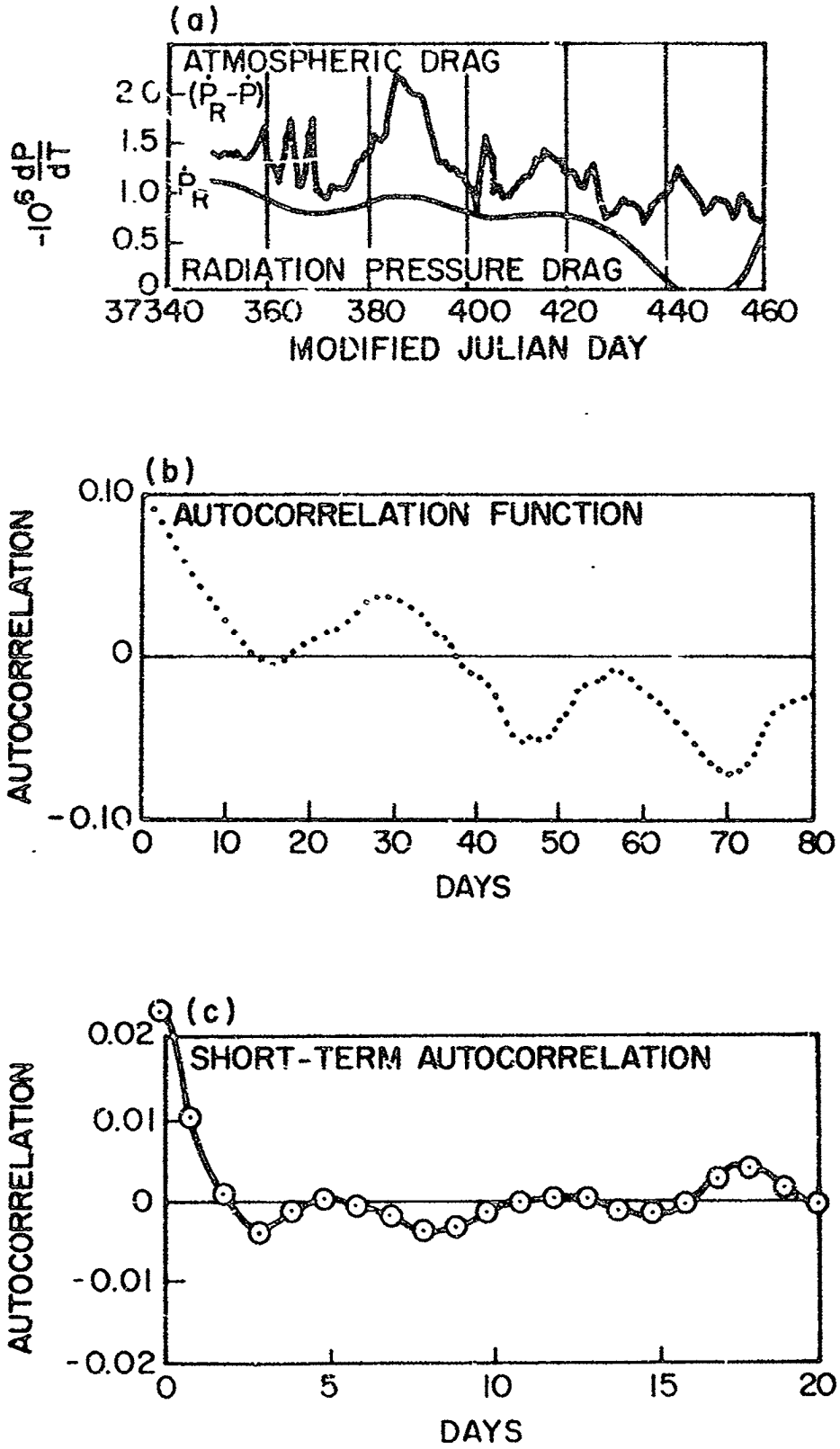

Figure 1 Atmospheric Drag And Autocorrelation Functions For EXPLORER IX.

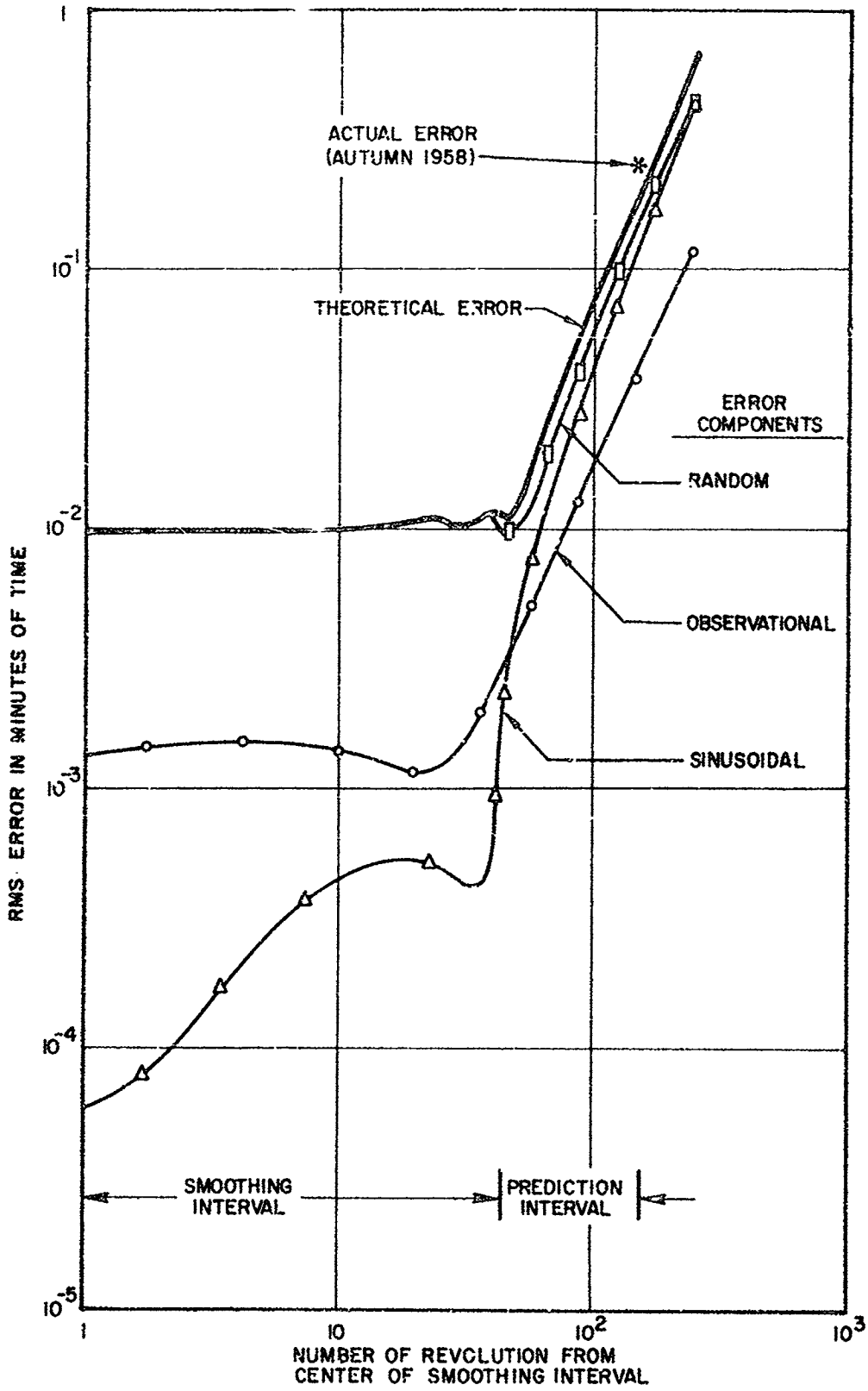

Figure 2 Error In Vanguard I Predictions Near Sunspot Maximum

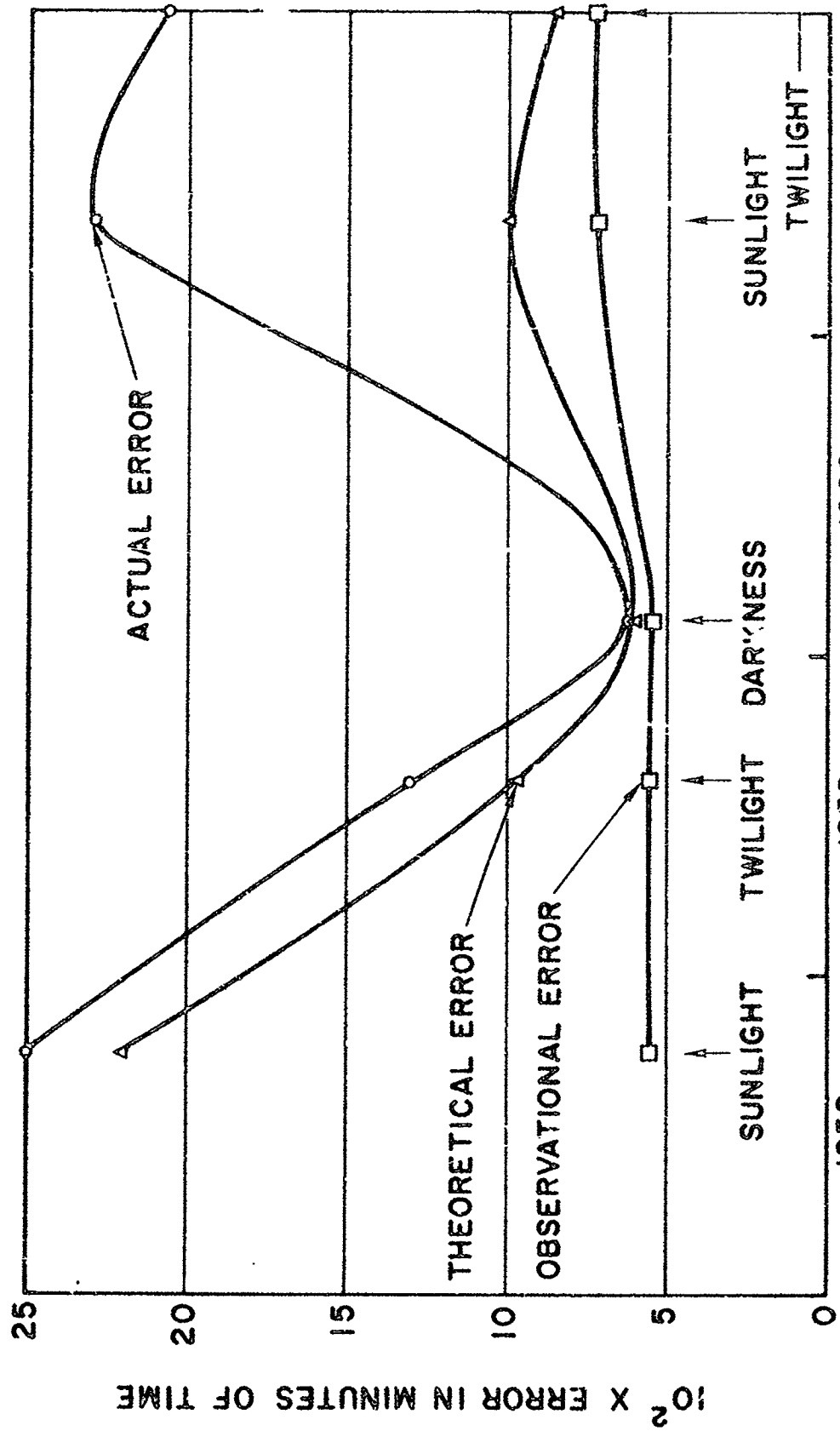

Figure 3 Error In One-to-Two Week Orbital Predictions For Vanguard I

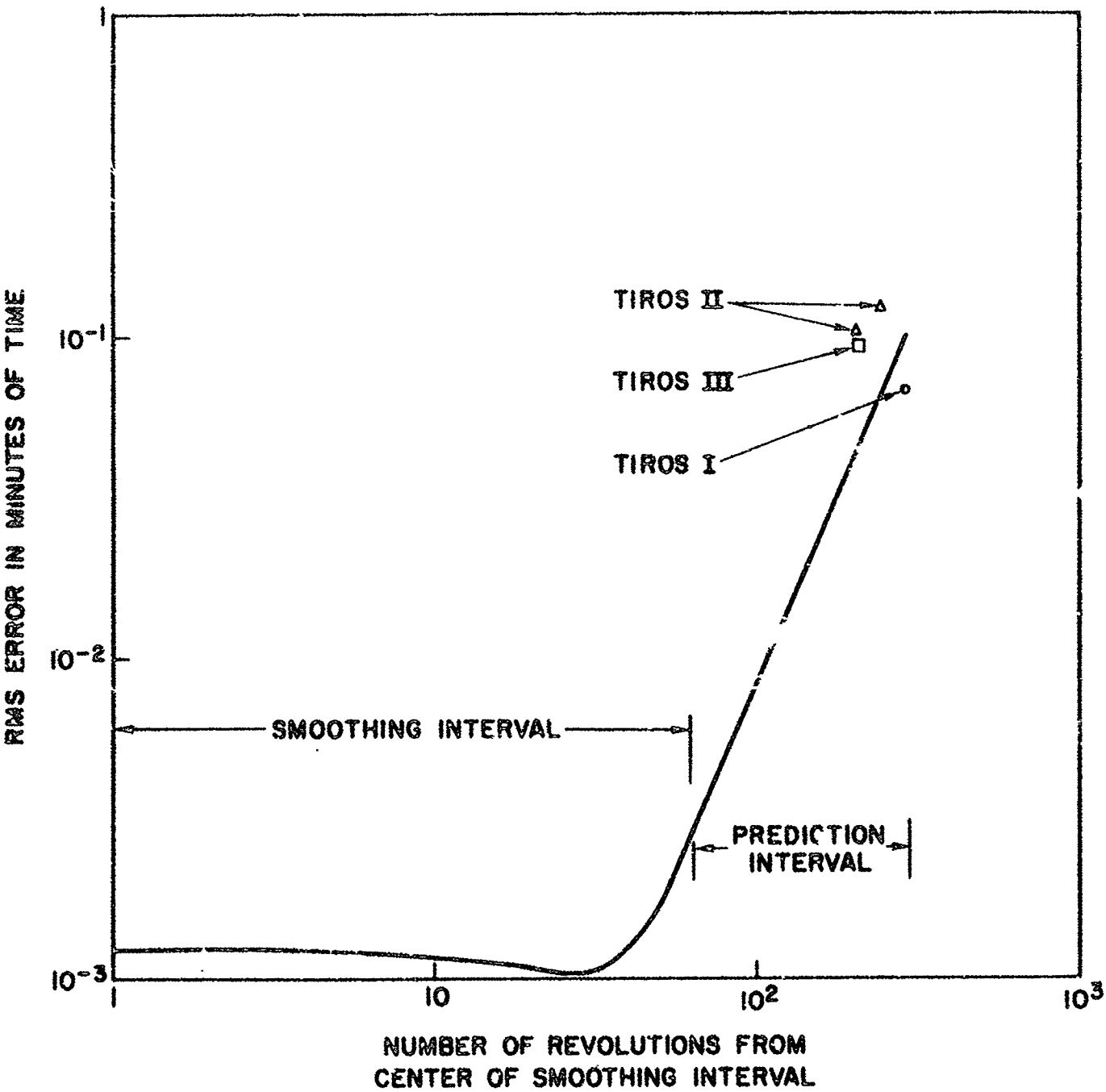

Figure 4 Tangential Error Of Orbital Predictions For Tiros Weather Satellites

PART II

APPENDIX 2

ON THE OPTIMUM CHOICE OF A SMOOTHING INTERVAL FOR COMPUTING DEFINITIVE ORBITS OF ARTIFICIAL SATELLITES*

by

Kenneth Moe

*Presented at the COSPAR-IAG Symposium on the Use of Artificial Satellites for Goedesy, Washington, April 26-28, 1962

INTRODUCTION

When orbits are computed for artificial earth satellites, it is found that there are erratic fluctuations in the orbital elements, in addition to the slow secular and periodic changes. These erratic fluctuations are caused partly by observational errors, and partly by fluctuations in air drag. In constructing definitive orbits for artificial satellites, one tries to make the best compromise between introducing unreal fluctuations due to observational errors, and concealing real fluctuations by doing too much smoothing. In order to devise a criterion for the optimum smoothing interval, one must first know something about the statistical properties of the fluctuations in air drag; therefore, we shall first investigate the autocorrelations of the fluctuations. Then we shall present a solution to the problem of choosing an optimum smoothing interval.

STATISTICAL PROPERTIES OF AIR DRAG

Some of the best data on satellite drag have been derived by Jacchia and Slowey. Figure 1a shows their values of the orbital acceleration of EXPLORER I (1), for the first of the four time intervals for which they computed accelerations. The autocorrelation function has been derived from these accelerations and is shown in figure 1b. The autocorrelation function, $R(\tau)$, of a time function, $y(t)$ is defined by

$$R(\tau) = \overline{y(t)\, y(t+\tau)} = \lim_{T\to\infty} \frac{1}{2T} \int_{-T}^{T} dt\; y(t)\, y(t+\tau).$$

The autocorrelation function (2,3) shows how well the values of a time function are correlated at any two times which are separated by the interval τ. Figure 1b reveals the 27-day period which is correlated with the motion of active regions across the solar disk, and a 4-day period which is believed by Jacchia and Slowey to be caused by precession of the angular momentum vector of the tumbling satellite. Figure 1c shows the "short-term autocorrelation function", which is obtained by removing 27-day and 4-day sine waves from the orbital acceleration.

Figure 2a shows the orbital acceleration of EXPLORER IX, also derived by Jacchia and Slowey (4). Since this satellite is a large balloon, it is strongly affected by radiation pressure. However, this effect has been removed, leaving the acceleration due to atmospheric drag in the upper curve of figure 2a. It is only atmospheric drag which is used to obtain the autocorrelation functions shown in figures 2b and 2c.* The 27-day period

*A careful examination of the orbital accelerations of EXPLORER IX reveals that the short-term autocorrelation functions are quite different during geomagnetically disturbed periods than during quiet periods. The short-term autocorrelation function in figure 2c can be regarded as a weighted mean of the two correlation functions.

appears in figure 2b, but there is no other periodicity, because EXPLORER I is spherical in shape.

The short-term autocorrelation functions in figures 1c and 2c indicate that short-term fluctuations in atmospheric density are correlated over one or two days. These correlation times are upper bounds because of the correlations which were introduced by the smoothing process employed in deriving the orbital accelerations. An attempt to arrive at a lower bound is currently being made. It is based on a comparison of the orbital accelerations of EXPLORER VI, which had only two perigee passages a day, with those of other satellites which were being tracked at the same time. Until a definite value for the lower bound has been determined, the correlation time of one or two days will be used.

ERRORS IN ORBITAL PREDICTIONS

In order to obtain a criterion for the optimum smoothing interval, we must determine how the drag fluctuations (for which we now have a model) produce errors in orbital computations. We can accomplish this by employing a theoretical model (5) for errors in orbital predictions. The reason for considering errors in orbital predictions, rather than

errors in a definitive orbit, is that in a fluctuating atmosphere the actual orbit is difficult to define whereas the errors in an orbital prediction can easily be determined.

It is difficult to derive a theoretical model for the errors in orbital predictions when the fluctuations are correlated; therefore, it would be desirable to be able to assume that the short-term fluctuations were uncorrelated from one perigee passage to the next, and make an appropriate adjustment to the amplitude of the experimentally determined fluctuations. The results of a calculation (6) comparing uncorrelated and correlated models are shown in figure 3 by curves a and b respectively for an orbit in which the elements are perfectly known at the epoch. The correlated model assumes that the short-term fluctuations are perfectly correlated over intervals of 25 revolutions (a commonly used smoothing interval) and uncorrelated from interval to interval. The ordinate in figure 3 is R(N)/F where R(N) is the r.m.s. error in an orbital prediction caused by short-term fluctuations in drag, and F is the r.m.s. fluctuation in drag from one orbital revolution to the next on the assumption that the fluctuations are independent from revolution to revolution. The abscissa N is the number of orbital revolutions measured from the epoch. The errors computed from the

correlated and uncorrelated models differ by a factor of 5 in the first revolution after the epoch but differ by less than 50% after 25 revolutions. A third model (curve 3c) for the errors in predictions with perfect initial elements has been derived from the data on EXPLORER I given by Jacchia and Slowey (1). This model includes the 4-day sine waves and the short-term autocorrelation functions, examples of which are shown in figures 1b and 1c. There were actually four time intervals for which accelerations of EXPLORER I were computed by Jacchia and Slowey. The cross-hatched region in curve 3c shows the range of errors for these four time intervals. The small initial errors in curves 3a, b and c cannot be attained in practice because the initial elements are not perfectly known, but must be obtained by smoothing. The errors which should be expected in practice are illustrated by curve 3d which gives the results of a more involved calculation (7) assuming uncorrelated fluctuations, and elements derived by smoothing over 24 revolutions. A comparison of the curves reveals that it makes little difference whether the short-term fluctuations are assumed to be correlated or not if the smoothing interval is at least as large as the correlation time.

Since it makes little difference whether the short-term fluctuations are assumed correlated or uncorrelated, the simpler uncorrelated case

is used in the model (5) for errors in orbital predictions. This model assumes that the errors in orbital predictions are caused by observational errors, O(N), by a 27-day sinusoidal variation in atmospheric density, S(N), and by the short-term fluctuations, R(N), which are assumed to be independent from revolution to revolution. The independent variable, N, denotes the number of revolutions after the center of the interval over which observations are smoothed to obtain the elements. The total r.m.s. error is $E(N) = \left\{ [O(N)]^2 + [S(N)]^2 + [R(N)]^2 \right\}^{1/2}$. The r.m.s. values of the observational, sinusoidal, and random errors are given by the following equations (5):

$$O(N) = \frac{\sigma_o}{i^2\sqrt{M}} \left\{ i^4 \left[\frac{M}{M+2} + \frac{16}{9}\left(\frac{M+2}{M}\right)^2 \right] + 32\,Ni \left[\frac{i^2}{3M} - \frac{4N^2}{M+2} \right] + 256\,N^4 + 16N^2 i^2 \left[\frac{M}{M+2} - \frac{8}{3}\left(\frac{M+2}{M}\right) - \frac{2M}{(M+2)^2} \right] \right\}^{1/2} \quad (1)$$

$$S(N) = \frac{A}{k^2} \sqrt{\frac{\alpha^2 + \beta^2}{2}} \quad (2)$$

where

$$\alpha = \cos(kN) - \frac{2}{ik}\sin\left(\frac{ik}{2}\right) + \frac{64}{i^3k}\left[N^2 - \frac{i(i+2)}{12}\right]\left[1 - \cos\left(\frac{ik}{4}\right)\right]\sin\left(\frac{ik}{4}\right)$$

$$\beta = \sin(kN) - kN + \frac{8N}{ik(i+2)}\left[\cos\left(\frac{ik}{2}\right) - 1 + \frac{i^2k^2}{8}\right]$$

and

$$R(N) = F\left\{\frac{N^3}{3} + 2\left(\frac{i}{4}\right)^3\left[\frac{64}{5}\left(\frac{N}{i}\right)^4 - 16\left(\frac{N}{i}\right)^3 + \left(\frac{N}{i}\right)^2\right]\right\}^{1/2}$$

for

$$N \geq i/2$$

where

i = the smoothing interval in revolutions,

M = the number of independent observations in the smoothing interval,

$A = 5.2\, h_p\, |D| \times 10^{-4}$,

h_p = perigee height in kilometers,

D = rate of change of period in minutes per revolution

$F = 3.1\, h_p \left|D\right| \times 10^{-3}$

σ_o = equivalent error of a single independent observation in minutes of time.

and

$k = (2\pi P/27)$ where P is the period in days.

THE OPTIMUM SMOOTHING INTERVAL

The errors in one to two week orbital predictions (8) for a large number of satellites as given by the theoretical model, and as calculated from the actual predictions are compared in figure 4.* The success of the model in describing the errors in orbital predictions encourages us to employ the model also to describe the errors at the end of the smoothing interval, which we wish to use in our criterion for the optimum smoothing interval. The optimum smoothing interval, i_o, is taken to be the number of revolutions for which the error at the end of the smoothing interval caused by observational errors alone is equal to an arbitrary constant B. times the combined errors caused by the random and

*The sloping line in figure 4 represents the errors when drag variations are the main cause of errors in predictions. The horizontal line applies where the observational errors of the Minitrack system are the dominant cause of errors.

sinusoidal variations, i.e.

$$O(N) = B\left[R^2(N) + S^2(N)\right]^{1/2},$$

where

$$N = i_o/2$$

On substituting for O(N), S(N), and R(N) from equations (1), (2) and (3), and letting $C \equiv (1/M)$ be a constant for th. tracking system, this criterion yields the expression

$$i_o^4 = 1.01 \times 10^3 \frac{C\sigma_o^2}{B^2F^2}\left[1 + \frac{A^2k^2i_o^3}{220F^2}\left(1 - .028i_o^2k^2\right)\right]^{-1} \quad (1$$

for

$$20 < i_o < 200.$$

The lower bound on i_o is necessitated by approximations used in deriving equation (3), while the upper bound is caused by truncation

errors in the expansion of the trigonometric functions. Within these bounds equation (4) can be solved by iteration.

An example of how the observational, random, and sinusoidal errors varied with the smoothing interval in the case of VANGUARD I with its perigee in darkness is shown in figure 5. The optimum smoothing interval was calculated by equation (4) to be 130 revolutions for this case, when B was chosen to be equal to one, and there was one independent Minitrack observation per revolution (C = 1). Two examples of what happens if a smoothing interval shorter or longer than the optimum is used are shown in figures 6 and 7 respectively. Figure 6 shows the acceleration of VANGUARD I smoothed over intervals of 44 revolutions when perigee was in darkness (9). The fact that the acceleration was highly erratic and frequently went to zero indicates that too short a smoothing interval was employed. According to equation (4) the optimum smoothing interval in this case was 130 revolutions. Figure 7 shows the atmospheric density derived from the rocket of SPUTNIK III. The density derived by Kolegov was smoothed in overlapping intervals of approximately one week (10). The optimum smoothing interval in this case is estimated to have been 20 revolutions. Many real fluctuations in atmospheric density were caused to disappear by the use of an excessively long smoothing

interval. On the other hand, King-Hele presumably had a small fraction of the number of observations of the SPUTNIK III rocket available to Kolegov, so the two to three day smoothing interval King-Hele employed probably was too short (11). It is hoped that in the future the extremes illustrated in figures 6 and 7 can be avoided by employing a smoothing interval appropriate to each particular case.

REFERENCES

1. Jacchia, L. G. and Slowey, J. W. Smithsonian Astrophysical Observatory Special Report No. 77. 1961.

2. Lawson, J. L. and Uhlenbeck, G. E. Threshold Signals. McGraw-Hill Book Co., New York, 1947.

3. James, H. M., Nichols, N. B. and Phillips, R. S. Theory of Servomechanisms. McGraw-Hill Book Co., New York 1947.

4. Jacchia, L. G. and Slowey, J. W. Smithsonian Astrophysical Observatory Special Report No. 84. 1962.

5. Moe, Kenneth. TR-60-0000-09145. Space Technology Laboratories, April 1960.

6. Supplement to Reference 5. December 1961.

7. Unpublished calculations using the methods given in Appendices D and G of Reference 5.

8. Moe, Kenneth. Nature 192, 151, 14 October 1961.

9. Smithsonian Astrophysical Observatory Special Report No. 40 (R). Page 8. May 1960.

10. Kolegov, G. A., ARS Journal Volume 32. Page 485 - 487. 1962. (Translation of Iskusstvenniye Sputniki Zemli, Volume 4, Page 31-34. 1960.)

11. King-Hele, D. G., Properties of the Atmosphere Revealed by Satellite Orbits. Royal Aircraft Establishment, Farnborough, England. 1959. (To be published in Progress in the Astronautical Sciences).

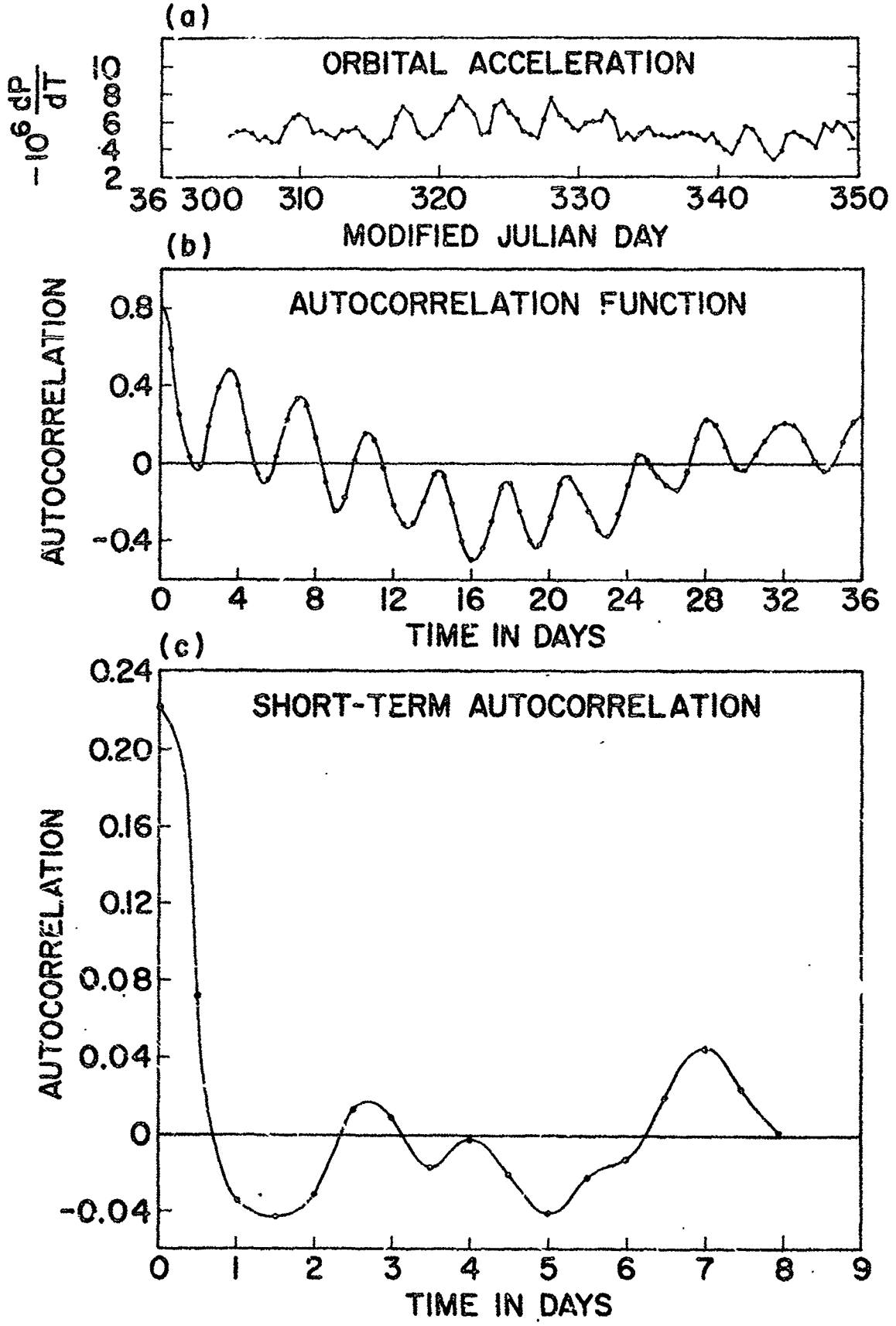

Figure 1. Orbital Acceleration and Autocorrelation Functions of EXPLORER I

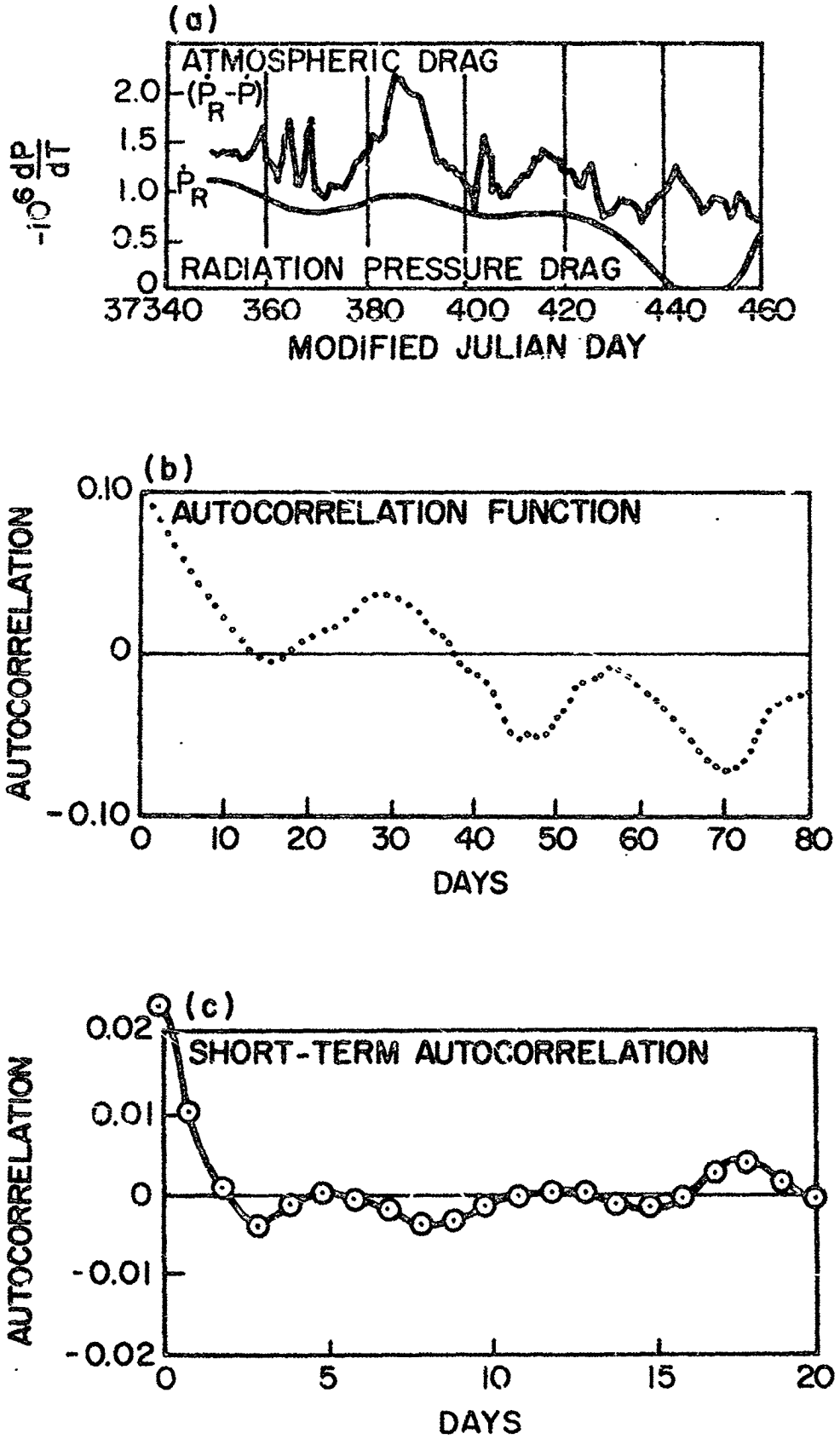

Figure 2. Orbital Acceleration and Autocorrelation Functions of EXPLORER IX

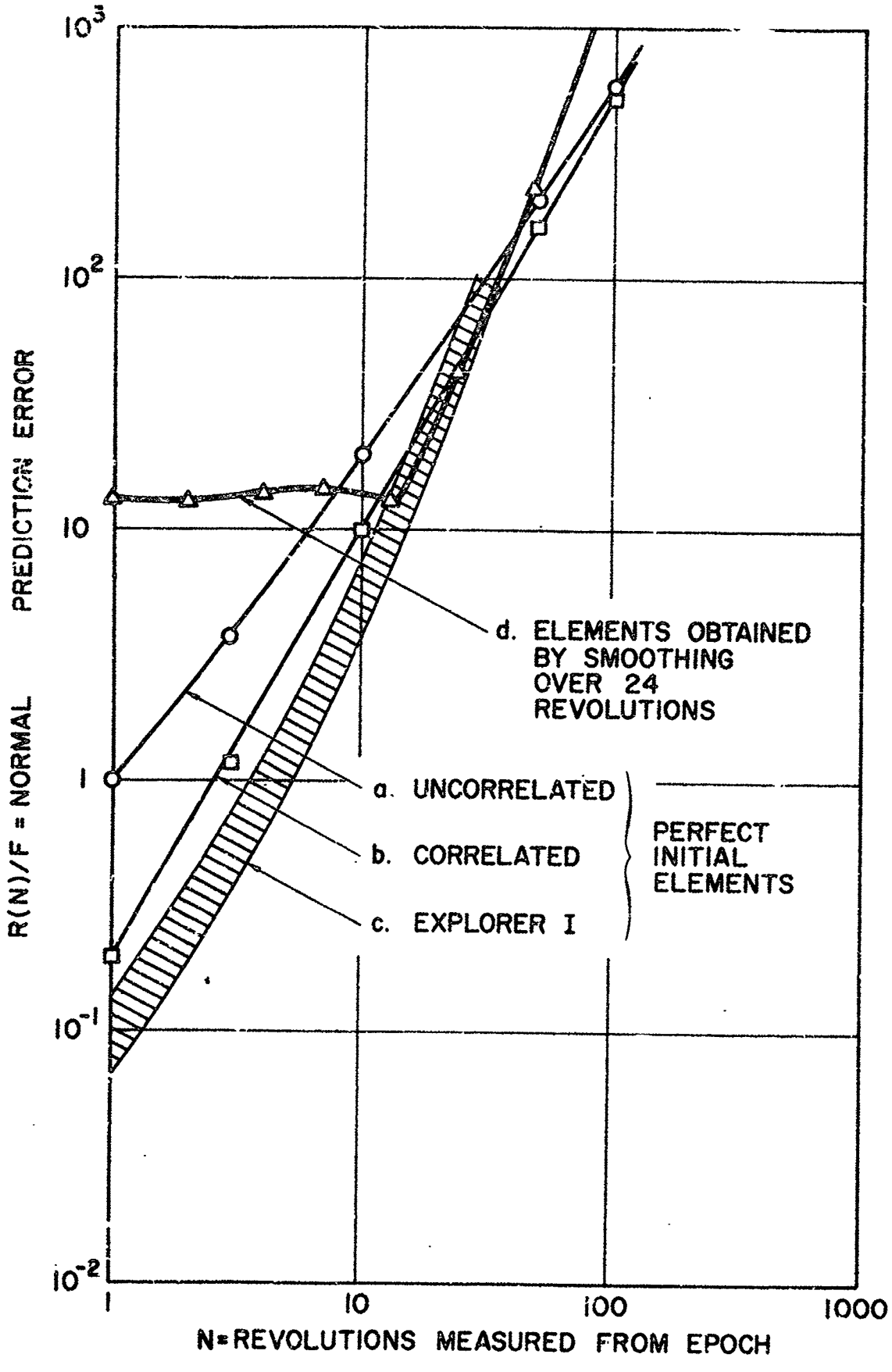

Figure 3. Errors in Orbital Predictions for Correlated and Uncorrelated Drag Fluctuations

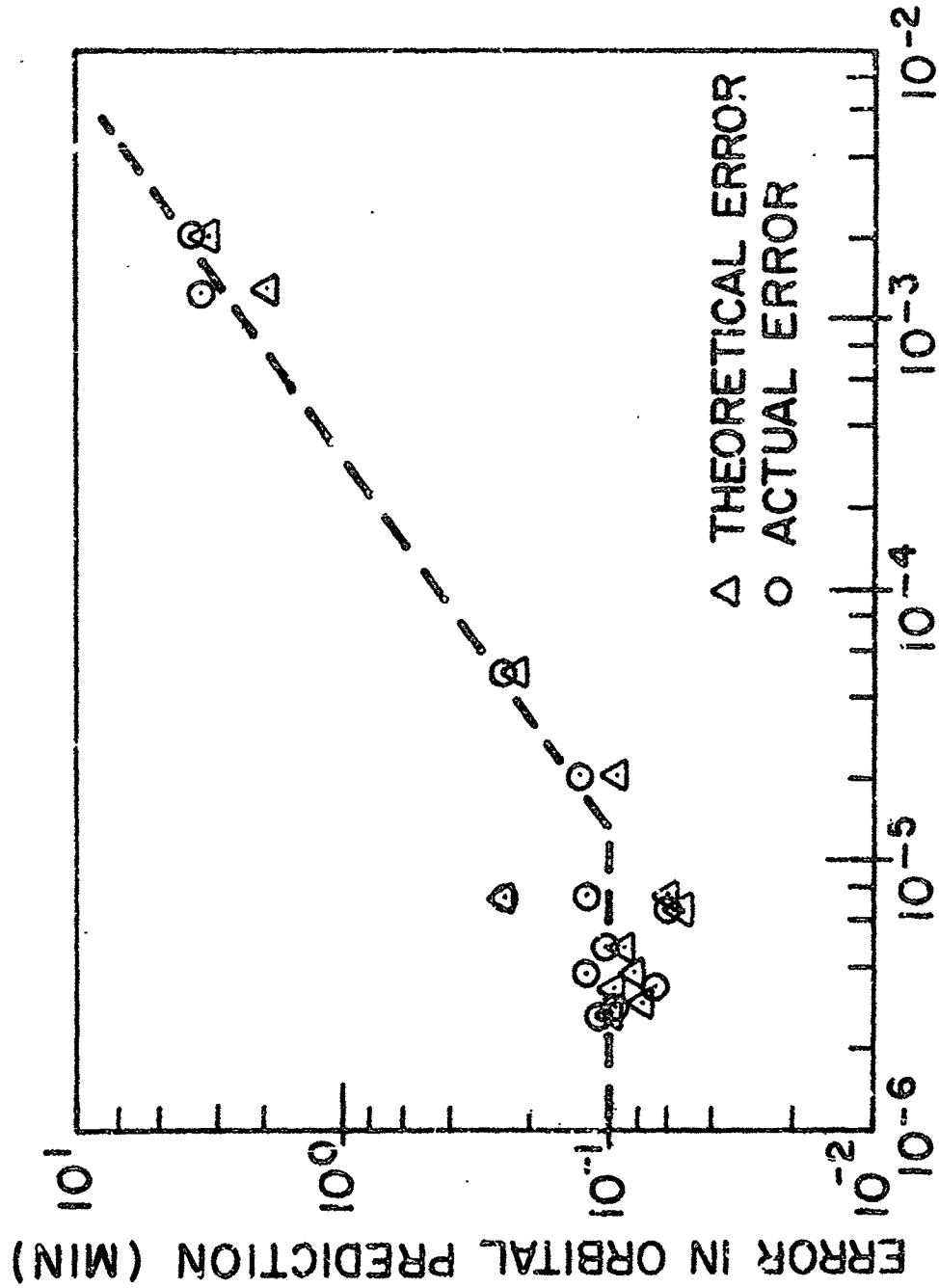

Figure 4. Errors in One-to-Two-Week Orbital Predictions

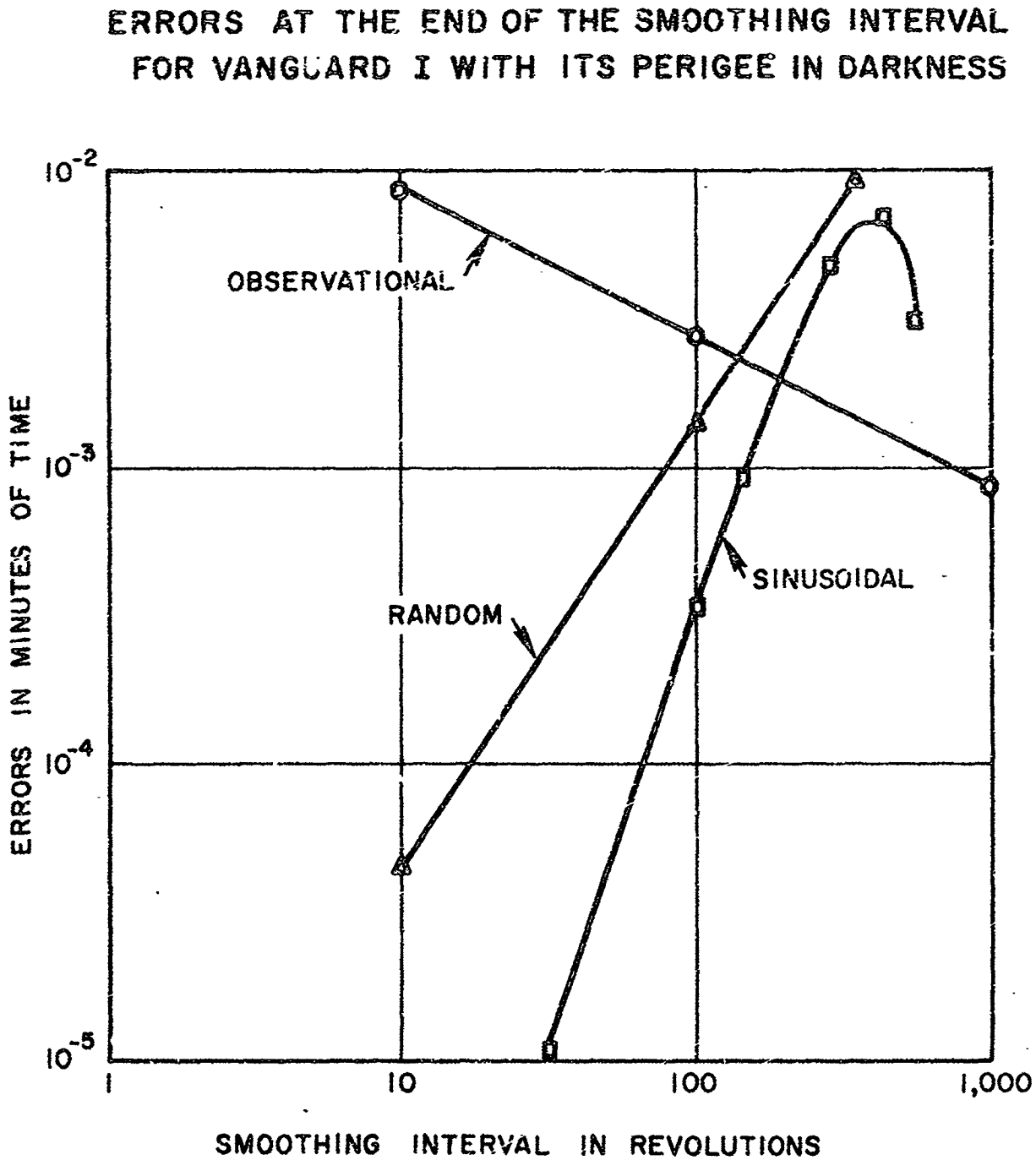

Figure 5. Errors at the End of the Smoothing Interval for VANGUARD I with its Perigee in Darkness

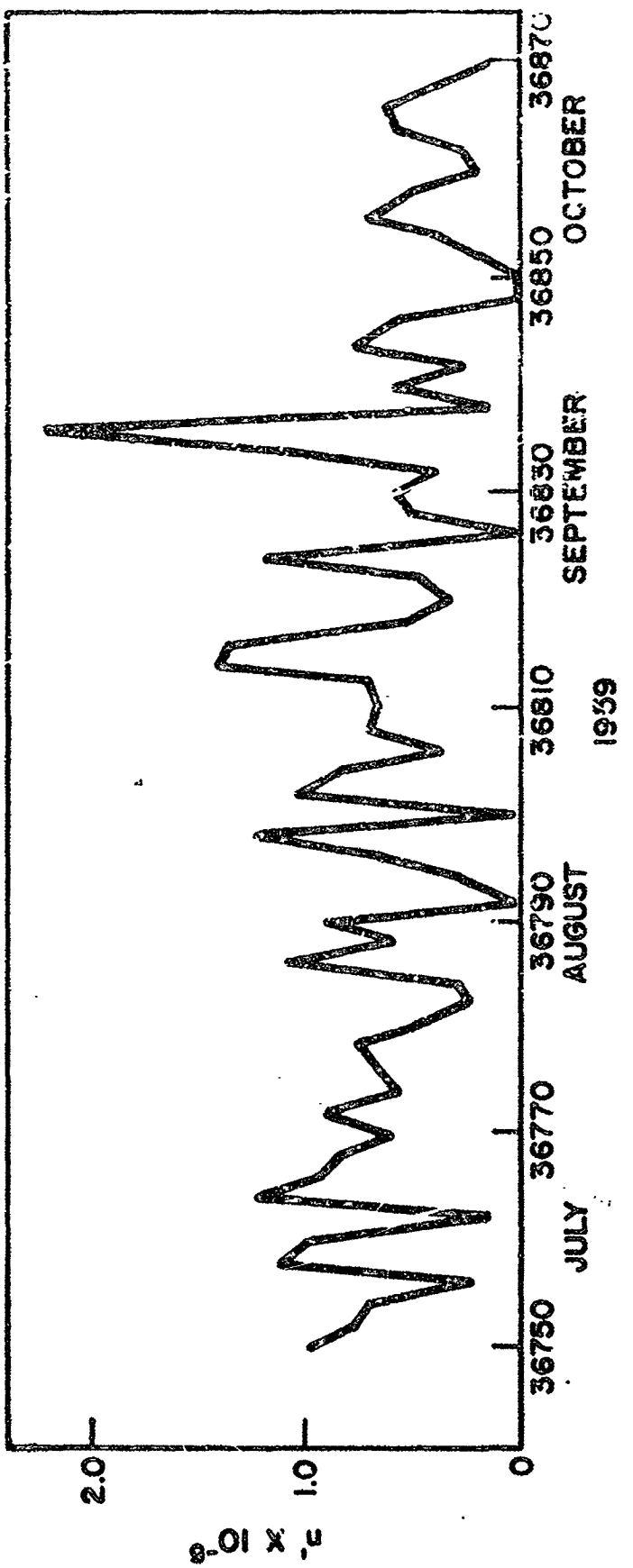

Figure 6. Orbital Acceleration of VANGUARD I Smoothed Over 4-Day Intervals

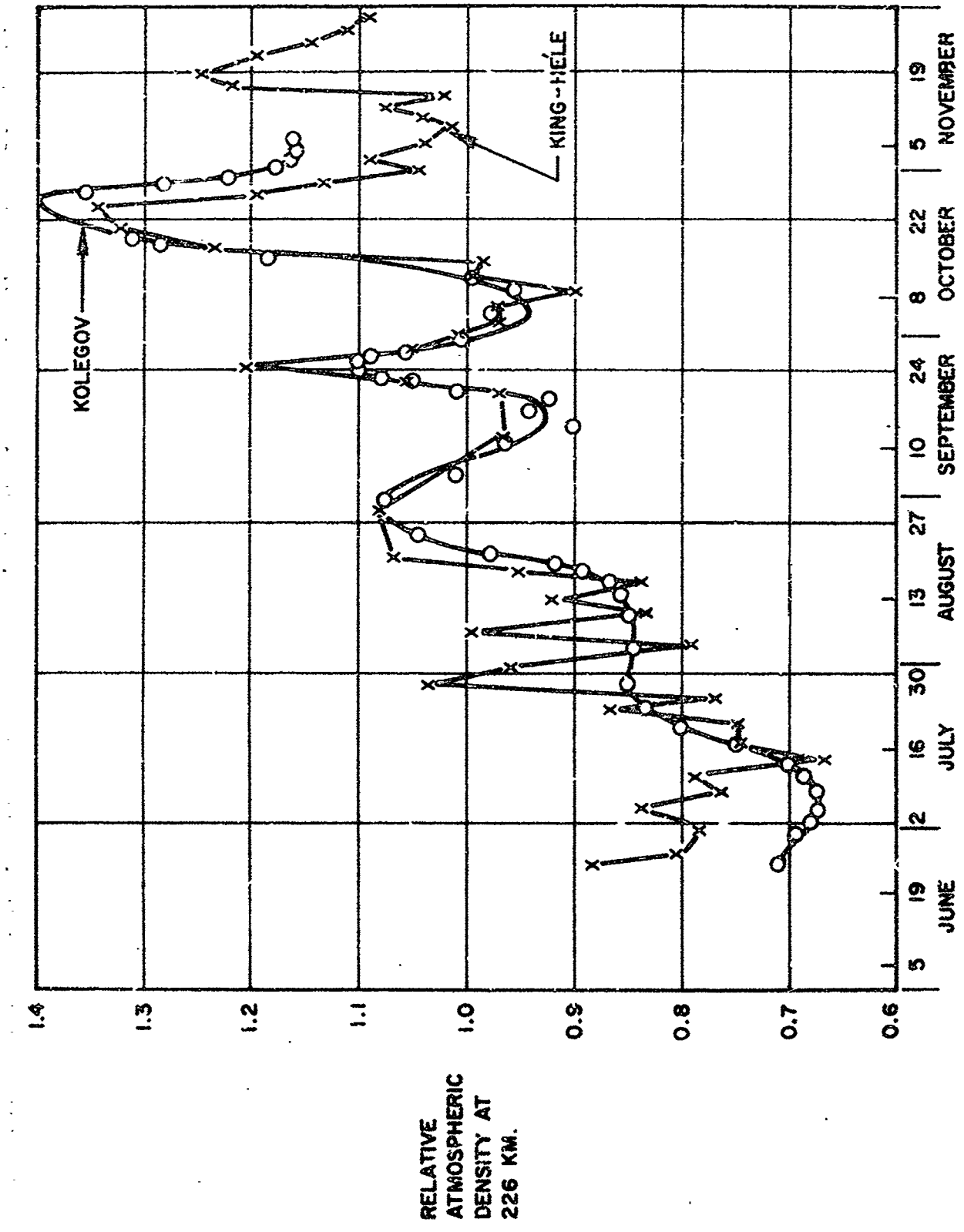

Figure 7. Relative Atmospheric Densities Derived From The Accelerations of The SPUTNIK III Rocket